(12) DeMore, W. B.; Margitan, J. J.; Molina, M. J.; Watson, R. T.; Hampson, R. F.; Kurylo, M. J.; Golden, D. M.; Howard, C. J.; Ravishankara, A. R. *Chemical Kinetics and Photochemical Data for Stratospheric Modeling; Evaluation No. 7.* Jet Propulsion Laboratory Publication No. 85-37 1985.
(13) Cantrell, C. H.; Shetter, R. E.; McDaniel, A. H.; Calvert, J. G. *J. Geophys. Res.* **1990**, *95*, 20531.
(14) Hammer, P. D.; Dlugokencky, E. J.; Howard, C. J. *J. Phys. Chem.* **1986**, *90*, 2491.
(15) Schiff, H. I.; Hastie, D. R.; Mackay, G. I.; Iguchi, T.; Ridley, B. A. *Environ. Sci. Technol.* **1983**, *17*, 352A.
(16) Chance, E. M.; Curtis, A. R.; Jones, I. P.; Kirby, C. R. FACSIMILE, Report R 8775; United Kingdom Atom Energy Authority, Harwell, 1977.
(17) Tyndall, G. S.; Orlando, J. J.; Cantrell, C. A.; Shetter, R. E.; Calvert, J. G. *J. Phys. Chem.* **1991**, *95*, 4381.
(18) Sander, S. P.; Kircher, C. C. *Chem. Phys. Lett.* **1986**, *126*, 149.
(19) Daniels, F.; Johnston, E. H. *J. Am. Chem. Soc.* **1921**, *43*, 53.
(20) Malko, M. W.; Troe, J. *Int. J. Chem. Kinet.* **1982**, *14*, 399.
(21) Kircher, C. C.; Margitan, J. J.; Sander, S. P. *J. Phys. Chem.* **1984**, *88*, 4370.
(22) Burrows, J. P.; Tyndall, G. S.; Moortgat, G. K. *Chem. Phys. Lett.* **1985**, *119*, 193.

A Study of the Reactions of H_3^+, H_2D^+, HD_2^+, and D_3^+ with H_2, HD, and D_2 Using a Variable-Temperature Selected Ion Flow Tube

Kevin Giles,*,† Nigel G. Adams,‡ and David Smith§

School of Physics and Space Research, University of Birmingham, Birmingham, B15 2TT, Great Britain
(Received: January 28, 1992; In Final Form: May 26, 1992)

The reactions of H_3^+ with H_2 in all possible deuterated combinations (i.e., H_3^+, H_2D^+, HD_2^+, and D_3^+ variously with H_2, HD, and D_2) have been studied at both 300 and 80 K using a VT-SIFT apparatus. The experimentally determined equilibrium constants are compared with those calculated using statistical mechanics. In general, the experimental and calculated equilibrium constants are in agreement at 300 K but differ significantly at 80 K. The discrepancy is considered in terms of nonequilibration of the reactant species at temperatures below 300 K in the VT-SIFT.

Introduction

The process of H/D isotope exchange in gas-phase ion–molecule reactions has been well studied from a fundamental standpoint[1-12] and toward gaining an understanding of heavy isotope enrichment in certain interstellar molecules.[13-26]

The process of H/D isotope exchange can be represented by the reaction

$$XH^+ + YD \underset{k_r}{\overset{k_f}{\rightleftharpoons}} XD^+ + YH - \Delta H \qquad (1)$$

where ΔH is the enthalpy change for the reaction and k_f and k_r are the forward (exothermic) and reverse (endothermic) rate coefficients, respectively. Since such a reaction only involves the interchange of isotopes, it is near thermoneutral and ΔH is essentially the difference between the zero-point vibrational energies of the products and reactants.

The equilibrium constant, K_{eq}, for reaction 1 is given by[27]

$$K_{eq} = k_f/k_r \qquad (2)$$

By using standard thermodynamic relationships, K_{eq} can be related to the enthalpy and entropy changes in a reaction by[28]

$$\ln\left(\frac{k_f}{k_r}\right) = -\frac{\Delta H}{RT} + \frac{\Delta S}{R} \qquad (3)$$

Hence, ΔH and ΔS for a reaction can be determined by measuring k_f and k_r as a function of temperature. A plot of $\ln(k_f/k_r)$ versus T^{-1} (a van't Hoff plot) yields ΔH from the gradient and ΔS from the intercept, assuming that ΔH and ΔS are essentially temperature invariant over the range studied.

The variation of the equilibrium constant with temperature can also be determined using statistical mechanics. It is readily shown for ground electronic and vibrational state species that[16,29]

$$K_{eq} = \left(\frac{\mu_p}{\mu_r}\right)^{3/2}\left(\frac{q_{p1}q_{p2}}{q_{r1}q_{r2}}\right)\exp\left(\frac{\Delta E}{k_B T}\right) \qquad (4)$$

where μ is the reduced mass and q the rotational partition function (including nuclear spin contributions) where the subscripts p and r refer to the products and reactants, respectively, and 1 and 2 distinguish the two products or reactants. ΔE is the zero-point energy released in the reaction ($\Delta E/k_B = -\Delta H/R$).

From expressions 3 and 4 it is apparent that at high temperatures, i.e., when $-\Delta H \ll RT$, the ratio k_f/k_r will be determined by the entropy change in the reaction. At lower temperatures, i.e., $-\Delta H > RT$, the enthalpy effects in the reaction become dominant; indeed, even at room temperature for a large $-\Delta H$ the reverse reaction can be significantly inhibited, favoring the incorporation of the heavy isotope into the ion. This effect is greatest for H/D exchange reactions due to the large mass difference between the isotopes (and hence large zero-point energy differences).

An interesting system in this context is the reaction of H_3^+ with H_2, in all of its deuterated analogues, since it is the simplest system without a chemical reaction channel in which multiple isotope labeling of both the ion and the neutral is possible. A particularly important reaction is

$$H_3^+ + HD \rightleftharpoons H_2D^+ + H_2 - \Delta H \qquad (5)$$

since this is a first step toward producing deuterated interstellar molecules. We have previously studied this reaction as a function of temperature using a variable-temperature selected ion flow tube apparatus (VT-SIFT).[13,17] Using expression 3, a $\Delta H/R = -(90 \pm 10)$ K was determined at 80 K. Using expression 4, Herbst calculated the variation of the equilibrium constant for this reaction as a function of temperature.[16] Good agreement was obtained between his calculated values of K_{eq} at 300 and 200 K and those determined experimentally. However, the calculated K_{eq} at 80 K was larger than the experimentally determined value. This discrepancy was explained by the fact that the species H_3^+, H_2D^+,

† Present address: Department of Chemistry, Montana State University, Bozeman, MT 59715.
‡ Present address: Department of Chemistry, University of Georgia, Athens, GA 30602.
§ Present address: Institut for Ionenphysik der Universitat Innsbruck, Technikerstrasse 25, A-6020 Innsbruck, Austria.

0022-3654/92/2096-7645$03.00/0 Published 1992 by the American Chemical Society

and H_2 do not reach true rotational equilibrium at low temperatures in the VT-SIFT apparatus, leaving them with sufficient suprathermal energy to drive the endothermic reverse reaction.[13,16,17] Because of this, the experimentally determined ΔH for reaction 5 was smaller than the calculated ΔH.

Reaction 5 forms one of a series of 10 reactions possible between deuterated forms of H_3^+ and H_2, namely H_3^+, H_2D^+, HD_2^+, and D_3^+ and H_2, HD, and D_2. Some of these 10 reactions have been reported previously by us;[9] however, we present here for the first time a complete study of these reactions at both 300 and 80 K. Additionally, the equilibrium constants for these reactions as determined from statistical mechanics (eq 4) are presented for the first time.

Experimental Section

The reactions reported here were studied with a variable-temperature selected ion flow tube (VT-SIFT) apparatus. This apparatus has been described in detail previously[30] and only a brief description is given here. Ions of interest are created in a remote ion source, selected using a quadrupole mass filter and injected through a venturi inlet into a fast flowing helium carrier gas. The ions are then convected along the flow tube by the helium to the detection system which consists of another quadrupole mass filter and a channeltron electron multiplier. Reactions are studied by adding neutral gas to the ion swarm upstream of the detection system. By monitoring the loss of the reactant ion and the formation of product ions as a function of reactant neutral density, we can obtain both the reaction rate coefficient and product ion distribution. To study reactions at 80 K, liquid nitrogen is circulated through coils around the flow tube.

The H_3^+ and D_3^+ ions were produced in a high-pressure electron impact ion source from H_2 and D_2, respectively, by the reactions

$$H_2^+ + H_2 \rightarrow H_3^+ + H \quad (6)$$

$$D_2^+ + D_2 \rightarrow D_3^+ + D \quad (7)$$

The partially deuterated ions H_2D^+ and HD_2^+ were produced by the reactions

$$H_2^+ + D_2 \rightarrow H_2D^+ + D,\ HD_2^+ + H \quad (8)$$

$$D_2^+ + H_2 \rightarrow H_2D^+ + D,\ HD_2^+ + H \quad (9)$$

using a mixture of H_2 and D_2 in the high-pressure ion source. Injection of these light ions into the helium carrier gas resulted in the production of HeH^+ and HeD^+ at 300 K and He_2H^+ and He_2D^+ at 80 K. These ions are produced by fragmentation of the injected ions to H^+ and D^+ which subsequently undergo association reactions with the helium carrier gas. Additionally, any residual internal energy in the injected ions may promote the endothermic proton-transfer reaction between the ions and helium atoms.

To reduce these effects, the ions were injected at low energy (<1 eV) and the ion source was operated at relatively high pressure to quench internal excitation of the ions. Under these conditions 10% fragmentation of H_3^+ occurred at 300 K and 40% fragmentation at 80 K. This residual fragmentation is believed to occur in the ion source quadrupole chamber where the relatively high potentials used on electrostatic lens elements supply the ions with sufficient energy to dissociate on the background helium gas that leaks in through the venturi inlet. More fragmentation occurs at 80 K because the venturi inlet is less efficient, thus resulting in a higher background helium concentration in the quadrupole chamber. The fragmentation of the other ions was less then for H_3^+, since their larger masses result in a lower center-of-mass collision energy on the helium. The HeH^+, HeD^+, He_2H^+, and He_2D^+ ions have to be accounted for in the data analysis since they react with H_2 and D_2 by proton transfer, producing the same ions as the reactions under study. Another potential problem arises if any vibrational excitation remains in the ions in the reaction region since this would effectively swamp the zero-point energy effects. The excess energy would be expected to drive the endothermic isotope-exchange reactions and be manifest as a nonlinear decay in a logarithmic plot of the reactant ion signal versus the concentration of the reactant neutral gas. However, no evidence for vibrational excitation was apparent in any of the present studies.

As mentioned in the Introduction, at lower temperatures in the VT-SIFT apparatus, it is believed that the reactant molecules do not attain a thermal rotational distribution.[13,17] This can be appreciated as follows; homonuclear molecules, such as H_2 and D_2 can have two different nuclear spin orientations, one with spins parallel (ortho) and one with spins antiparallel (para). The overall symmetry requirements for the molecular wave functions of these species place restraints on the rotational levels, J, which can be combined with a particular nuclear spin orientation. As a consequence, the ortho-H_2 molecules can only access odd-J rotational levels and the para-H_2 molecules only even-J levels, whereas for D_2 the opposite is the case. The ortho and para levels have different statistical weights in accordance with their different nuclear spins. For H_2 the ortho and para levels have nuclear spin statistical weights of 3 and 1, respectively, whereas for D_2 the ortho and para levels have statistical weights of 6 and 3, respectively. It has been shown experimentally, through studies of the heat capacities of H_2 and D_2, that interconversion between ortho and para spin states occurs only very slowly unless the gas is in contact with a paramagnetic surface.[31,32] Under equilibrium conditions at 300 K the number of molecules in the ortho and para spin states are approximately equal to the respective statistical weights of the levels, i.e., 3/4 of H_2 molecules are ortho and 1/4 are para, whereas for D_2, 2/3 are ortho and 1/3 are para. H_2 and D_2 in these respective populations are known as "normal". At 80 K (the lowest temperature used in the study), their respective ortho:para populations would eventually equilibrate to 1:1 and 2.3:1. However, as stated earlier, conversion between nuclear spin states is not facile and it is expected that at 80 K in the VT-SIFT experiment the H_2 and D_2 will have their normal ortho:para populations. Thus, in effect, the molecules have rotational energy at 80 K in excess of their equilibrium values which can influence these near-thermoneutral reactions. Since HD is heteronuclear, there are no ortho/para states and it is expected to equilibrate fully in the VT-SIFT.

The H_3^+-like ions also have different nuclear spin orientations and it is likely that they are produced in their normal distribution in the "hot" ion source. Although it cannot be substantiated, it seems plausible that interconversion between the nuclear spin states of the ions will be inefficient in the carrier gas and they will also possess excess energy at low temperatures.

All of the reactions were studied at helium gas pressures of 0.61 Torr at 300 K and 0.28 Torr at 80 K. The rate coefficients and product ion distributions are estimated to be accurate to ±25% and ±5 in the percentage value, respectively. However, relative errors between the rate coefficients are estimated to be ±10% and thus the experimentally determined K_{eq} are thought to be accurate to ±15%.

Results and Discussion

The measured rate coefficients and product ion distributions for the reactions in the $H_3^+ + H_2$ system at 300 and 80 K are listed in Table I, together with the enthalpies of the reactions (as calculated from zero-point energies[33,34]) and the respective Langevin collision rate coefficients. Those reactions studied by us previously have been reinvestigated here and are included in the table and discussions for the sake of completeness. The present data are in good agreement with those reported by us previously. The kinetic data in Table I provide the information necessary to determine the forward and reverse rate coefficients k_f and k_r, respectively, for all possible combinations of reactions in the $H_3^+ + H_2$ system. For example, reaction iva in Table I is the reverse of reaction iiia, and the corresponding k_f and k_r are determined by multiplying the overall measured rate coefficients for reactions iii and iv by the relative fractions of the products in channels iiia and iva, respectively. The k_f and k_r determined in this way are listed in Table II. Equilibrium constants, K_{eq}, determined from the ratio k_f/k_r (see eq 2) are also reported in Table II. The validity of determining values of K_{eq} in this manner for the $H_3^+ + H_2$

TABLE I: Rate Coefficients (k)[a] and Product Ion Percentages (%) for Reactions in the $H_3^+ + H_2$ System at 80 and 300 K

	reaction[b]	$\Delta E/k_B$ (K)	80 K k ($cm^3\ s^{-1}$)	80 K %	300 K k ($cm^3\ s^{-1}$)	300 K %	k_c[c] ($cm^3\ s^{-1}$)
i	[4] $H_3^+ + HD \rightarrow H_2D^+ + H_2$ [6]	+143	1.2(−9)	100	9.6(−10)	100	1.7(−9)
ii	[6] $H_2D^+ + H_2 \rightarrow H_3^+ + HD$ [4]	−143	3.2(−10)	100	5.3(−10)	100	1.8(−9)
iii[a]	[1] $H_3^+ + D_2 \rightarrow H_2D^+ + HD$ [6]	+63	1.4(−9)	25	1.3(−9)	20	1.6(−9)
iii[b]	$HD_2^+ + H_2$ [3]	+251		75		80	
iv[a]	[6] $H_2D^+ + HD \rightarrow H_3^+ + D_2$ [1]	−63	8.5(−10)	5	5.0(−10)	10	1.6(−9)
iv[b]	$HD_2^+ + H_2$ [3]	+187		95		90	
v[a]	[3] $HD_2^+ + H_2 \rightarrow H_3^+ + D_2$ [1]	−251	6.0(−10)	20	7.6(−10)	25	1.8(−9)
v[b]	$H_2D^+ + HD$ [6]	−187		80		75	
vi[a]	[3] $H_2D^+ + D_2 \rightarrow HD_2^+ + HD$ [6]	+107	1.4(−9)	50	1.0(−9)	65	1.5(−9)
vi[b]	$D_3^+ + H_2$ [1]	+341		50		35	
vii[a]	[6] $HD_2^+ + HD \rightarrow H_2D^+ + D_2$ [3]	−107	8.0(−10)	20	4.5(−10)	75	1.5(−9)
vii[b]	$D_3^+ + H_2$ [1]	+234		80		25	
viii[a]	[1] $D_3^+ + H_2 \rightarrow H_2D^+ + D_2$ [3]	−341	5.2(−10)	30	8.2(−10)	65	1.7(−9)
viii[b]	$HD_2^+ + HD$ [6]	−234		70		35	
ix	[6] $HD_2^+ + D_2 \rightarrow D_3^+ + HD$ [4]	+154	8.7(−10)	100	5.2(−10)	100	1.4(−9)
x	[4] $D_3^+ + HD \rightarrow HD_2^+ + D_2$ [6]	−154	5.0(−10)	100	6.6(−10)	100	1.5(−9)

[a] Absolute errors of ±25% are placed on the measured rate coefficients, although the relative values are expected to have smaller errors associated with them (±10%). ΔE represents the zero-point energy released in the reaction (including the rotational zero-point-energy of H_3^+ where appropriate) and k_B is the Boltzmann constant. Rate coefficients in the form $a(-b)$ are used to represent $a \times 10^{-b}$. [b] The quantities in square brackets are the probabilities of producing the respective $H_3^+ + H_2$ combination from a fully mixed $(H_5^+)^*$-like complex. [c] k_c is the Langevin collision rate coefficient.

TABLE II: Forward and Reverse Rate Coefficients (k_f and k_r ($cm^3\ s^{-1}$), Respectively)[a] for the Reactions in the $H_3^+ + H_2$ System at 80 and 300 K Together with Equilibrium Constants Calculated Experimentally, k_f/k_r, and Using Statistical Mechanics, K_{eq}

reaction[b]	k_f/k_r 80 K	k_f/k_r 300 K	80 K k_f/k_r[c]	80 K K_{eq}	300 K k_f/k_r[c]	300 K K_{eq}
$H_3^+ + HD \rightarrow H_2D^+ + H_2$ $H_2D^+ + H_2 \rightarrow H_3^+ + HD$	1.2(−9) 3.2(−10)	9.6(−10) 5.3(−10)	3.8	6.6	1.8	2.0
$H_3^+ + D_2 \rightarrow H_2D^+ + HD$ $H_2D^+ + HD \rightarrow H_3^+ + D_2$	3.5(−10) 4.3(−11)	2.6(−10) 5.0(−11)	8.2	13.2	5.2	6.7
$H_3^+ + D_2 \rightarrow HD_2^+ + H_2$ $HD_2^+ + H_2 \rightarrow H_3^+ + D_2$	1.1(−9) 1.2(−10)	1.0(−9) 1.9(−10)	9.2	48.3	5.3	5.1
$H_2D^+ + HD \rightarrow HD_2^+ + H_2$ $HD_2^+ + H_2 \rightarrow H_2D^+ + HD$	8.1(−10) 4.8(−10)	4.5(−10) 5.7(−10)	1.7	3.6	0.8	0.8
$H_2D^+ + D_2 \rightarrow HD_2^+ + HD$ $HD_2^+ + HD \rightarrow H_2D^+ + D_2$	7.0(−10) 1.6(−10)	6.5(−10) 3.4(−10)	4.4	7.2	1.9	2.5
$H_2D^+ + D_2 \rightarrow D_3^+ + H_2$ $D_3^+ + H_2 \rightarrow H_2D^+ + D_2$	7.0(−10) 1.6(−10)	3.5(−10) 5.3(−10)	4.4	14.5	0.7	0.8
$HD_2^+ + HD \rightarrow D_3^+ + H_2$ $D_3^+ + H_2 \rightarrow HD_2^+ + HD$	6.4(−10) 3.6(−10)	1.1(−10) 2.9(−10)	1.8	2.0	0.4	0.3
$HD_2^+ + D_2 \rightarrow D_3^+ + HD$ $D_3^+ + HD \rightarrow HD_2^+ + D_2$	8.7(−10) 5.0(−10)	5.2(−10) 6.6(−10)	1.7	4.0	0.8	1.0

[a] Rate coefficients in the form $a(-b)$ are used to represent $a \times 10^{-b}$. [b] For each pair of reactions, k_f relates to the first (forward) reaction and k_r relates to the second (reverse) reaction. [c] Errors of ±15% apply to the experimentally determined equilibrium constants.

system of reactions is discussed later.

Kinetics. In the $H_3^+ + H_2$ system of reactions, two different mechanisms are possible: one is the direct proton or deuteron transfer from the ion to the neutral molecule which can occur through a short-lived weakly bound $(H_5^+)^*$-like intermediate complex; the other is the process of H/D exchange between the ion and the neutral molecule which requires a longer lived $(H_5^+)^*$-like intermediate complex. The latter process of H/D exchange may possibly occur through successive H^+/D^+ shuttling in the long-lived complex, for example,

$$H_3^+ + D_2 \rightleftharpoons H_3^+{\cdot}D_2 \underset{H^+}{\overset{H^+}{\rightleftharpoons}} H_2{\cdot}HD_2^+ \underset{D^+}{\overset{D^+}{\rightleftharpoons}} H_2D^+{\cdot}HD \qquad (10)$$

$$\downarrow \qquad\qquad \downarrow$$

$$H_2 + HD_2^+ \qquad H_2D^+ + HD$$

Isotope exchange through H^+/D^+ shuttling has been considered in more detail by Henchman et al.[35] Of the 10 reactions listed in Table I, four can only produce a single product ion, whereas, for the remaining six, two product ions are possible. It should be noted also that regeneration of the reactant species can occur from the $(H_5^+)^*$-like complex and in some cases through H^+ or D^+ transfer; this is manifest as a measured rate coefficient which is less than the collision-limiting (Langevin) value. The statistical distributions for reactant and product channels listed in Table I are those expected from a purely random production of the observed species from a fully mixed $(H_5^+)^*$-like complex, i.e., where enthalpic effects are not important.

Of the four reactions which produce only one product, reactions i and ix in Table I are calculated to be exothermic and their reverse reactions, ii and x, endothermic. The reactions can occur by both direct H^+/D^+ transfer or by H/D exchange. The rate coefficients for both reactions i and ix are observed to increase with decreasing temperature. For the endothermic reactions, ii and x, as expected, the rate coefficients decrease with decreasing temperature. The rate coefficient for reaction i has been estimated previously by Huntress and Anicich to be 3×10^{-10} $cm^3\ s^{-1}$ using ICR data,[36] a value somewhat smaller than the present results, which may be due to the suprathermal energies of the ions in the ICR cell.

Reactions iii and vi occur via two exothermic channels and the overall rate coefficients are observed to increase slightly with decreasing temperature. At 300 K the HD_2^+ product is favored in both reactions. In both cases, this ion can be produced by direct

H^+ transfer and additionally by H/D exchange in reaction vi where it is the statistically favored product. Interestingly, the measured product distribution in reaction vi is similar to that expected statistically by direct H^+ or D^+ transfer from the reactant H_2D^+ ion. At 80 K, enthalpic effects become more dominant, increasing the fraction of the more exothermic D_3^+ product ion in reaction vi and maintaining the dominance of the more exothermic HD_2^+ product ion in reaction iii. In the merged beam studies of Gentry[3] for reaction iii, only the direct H^+-transfer product was detected as expected, since the higher ion energies of this experiment reduce the complex lifetime such that H/D exchange is not efficient.

The product channels in reactions v and viii are all endothermic and, accordingly, the overall reaction rate coefficients decrease with decreasing temperature. Notably, the statistically favored and less endothermic H_2D^+ product ion in reaction v is dominant at both 80 and 300 K and can be produced both by D^+ transfer or H/D exchange. The direct D^+-transfer product ion, H_2D^+, is favored in reaction viii at 300 K, indicating that only a short-lived intermediate complex is formed. However, at 80 K, enthalpic effects are more important and the less endothermic HD_2^+ product ion, resulting from H/D-exchange dominates. The tandem ICR result of Smith and Futrell[2] for reaction viii indicates essentially the same product ion distribution as the present 300 K data; that the reported rate coefficient is approximately half of the present value may be accounted for as before by suprathermal energies of the ions in the ICR cell.

Exothermic and endothermic channels are possible for reactions iv and vii; notably, the overall reaction rate coefficients increase with decreasing temperature to half of the Langevin rate coefficient. This indicates that significant regeneration of the reactant ions is occurring through H^+ and D^+ transfer in both reactions. As might be expected, the HD_2^+ product ion dominates at both 300 and 80 K in reaction iv since it is statistically favored and exothermic and can occur by direct D^+ transfer. Significantly, in an ICR study of reaction iv, only the HD_2^+ product ion was observed and a rate coefficient of 2.6×10^{-10} cm^3 s^{-1} was reported, again, the difference with the present results possibly being due to suprathermal ion energies in the ICR cell.[1] The endothermic channel to the H_2D^+ product ion is favored at 300 K in reaction vii since it is statistically favored and can be produced by direct H^+ transfer. At 80 K, enthalpic effects are more important and the exothermic channel producing D_3^+ ions by H/D exchange is dominant. Again, in an ICR study, only the direct H^+-transfer product, H_2D^+, was observed in reaction vii, and the reaction rate coefficient, 3.5×10^{-10} cm^3 s^{-1},[1] is somewhat less than the present VT-SIFT result. The merged beam studies of Gentry[3] indicated both product channels to be present in reaction vii at low energies; however, the D_3^+ product ion was a minor channel and decreased with increasing ion energy.

Equilibrium Constants. The determination of the thermodynamic quantities ΔH and ΔS for a reaction using a van't Hoff plot was mentioned in the Introduction. The forward and reverse rate coefficients listed in Table II have been used to calculate the equilibrium constant, K_{eq} ($=k_f/k_r$), for each reaction at 300 and 80 K. These K_{eq} values are listed in Table II. The use of a van't Hoff plot to determine ΔH and ΔS is only valid if these quantities are temperture invariant, a condition which is not satisfied in the $H_3^+ + H_2$ system of reactions as discussed below.

In isotope-exchange reactions, it is generally considered that ΔH for the reaction is given by the difference between the zero-point vibrational energies of the products and reactants. However, another important factor in the $H_3^+ + H_2$ system of reactions is the rotational energy content of the species. For these molecules, the equipartition theory does not adequately describe the energy content per rotational mode due to their large rotational energy level spacing (of the order of k_BT). To accurately calculate the rotational energy content, E_{rot}, of these species requires the use of partition functions. E_{rot} is given by the expression[37]

$$E_{rot} = k_B T^2 \frac{\delta \ln (q_{r-n})}{\delta T} \qquad (11)$$

TABLE III: Critical Data Used in the Calculation of the Rotational Partition Functions for H_3^+, H_2, and their Deuterated Analogues

molecular species	zero-point vibrnl energy (eV)	ref	rotatnl const (cm^{-1})	ref
H_2	0.2691	33	59.322	33
HD	0.2336	33	44.662	33
D_2	0.1912	33	42.992	33
H_3^+	0.54107	34	*a*	39
H_2D^+	0.49322	34	*a*	40
HD_2^+	0.44156	34	*a*	41
D_3^+	0.38588	34	*a*	42

[a] The energies of the rotational levels were obtained from the references listed.

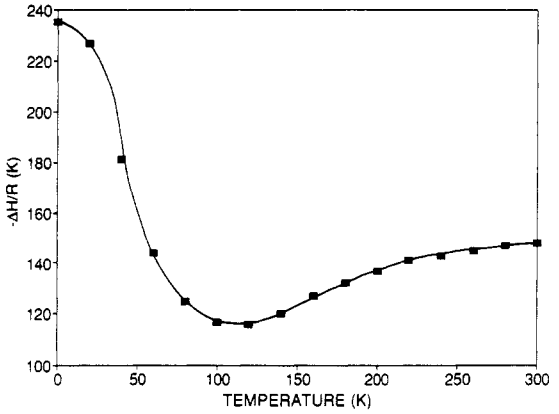

Figure 1. Calculated values of $\Delta H/R$ at different temperatures for the reaction $H_3^+ + HD \rightleftharpoons H_2D^+ + H_2$ as derived from zero-point energies and rotational energy contents of the species using eq 13. These data assume that the nuclear spin states of the species are equilibrated to the kinetic temperature.

where q_{r-n} is the combined rotational and nuclear spin partition function of the molecule which is in turn given by[38]

$$q_{r-n} = \sum g_J \exp\left(-\frac{\epsilon_J}{k_B T}\right) \qquad (12)$$

ϵ_J is the energy of the Jth rotational level and g_J is the statistical weight. The derivation of the q_{r-n} for the H_3^+- and H_2-like species requires a knowledge of the rotational energy level spacings and the degeneracy of each level. Fortunately, such data are available from spectroscopic studies of the species and calculations and these are presented in Table III.

The overall enthalpy change, ΔH, in a reaction is thus given by

$$\frac{\Delta H}{R} = \frac{\Delta E_{rot}}{k_B} - \frac{\Delta E}{k_B} \qquad (13)$$

where ΔE_{rot} is the rotational energy difference between the product and reactant species and ΔE is the zero-point energy released in the reaction. An additional factor must be taken into account at this point for reactions involving H_3^+ ions. The geometry and nuclear spin of this ionic species renders the ground rotational level inaccessible in accordance with the Pauli exclusion principle.[43] Thus the effective ground rotational state $H_3^+(J=1, K=1)$ lies 92.5 K above the true ground state $H_3^+(J=0, K=0)$.[39] This rotational zero-point energy can be treated in the same way as the vibrational zero-point energy of the species and is included in ΔE where appropriate.

The variation of ΔE_{rot} with temperature is significant compared to ΔE and this makes ΔH quite temperature dependent. We have previously presented the variation of ΔH with temperature for reaction 5;[17] however, more accurate spectroscopic data and calculations are now available on the molecular ions and so we report the new calculated values of ΔH in Table IV as deduced from the data in Table III. Figure 1 illustrates the data graphically. As can be seen, $\Delta H/R$ varies markedly with temperature, dropping from −148 K (essentially $-\Delta E/k_B$) at 300 K to a min-

TABLE IV: Calculated Enthalpy Changes (ΔH) for the $H_3^+ + HD \rightleftharpoons H_2D^+ + H_2$ Reaction as a Function of Temperature Assuming Equilibrium Nuclear Spin Distributions

temp (K)	rotatnl energy content, E_{rot}/k_B (K)				$\Delta E_{rot}/k_B$[a] (K)	$\Delta H/R$[b] (K)
	H_3^+	HD	H_2D^+	H_2		
0	92	0	0	0	-92	-235
20	101	1	18	0	-84	-227
40	111	14	68	19	-38	-181
60	122	36	98	59	-1	-144
80	138	57	123	90	18	-125
100	157	77	149	111	26	-117
120	180	98	178[c]	127	27	-116
140	206	118	206*	141	23	-120
160	234	138	234*	154	16	-127
180	263	158	263*	169	11	-132
200	292	178	292*	184	6	-137
220	322	198	322*	200	2	-141
240	352	218	352*	218	0	-143
260	382	238	382*	236	-2	-145
280	412	258	412*	254	-4	-147
300	443	278	443*	273	-5	-148

[a] $\Delta E_{rot} = E_{rot}(H_2D^+) + E_{rot}(H_2) - E_{rot}(H_3^+) - E_{rot}(HD)$. [b] $\Delta H/R$ is calculated using eq 13 in the text with $\Delta E/k_B = 143$ K. [c] No data were available on the higher energy rotational levels of H_2D^+, thus preventing the calculation of $E_{rot}(H_2D^+)$ above 100 K. However, at higher temperatures, the quantum effects are less important and $E_{rot}(H_2D^+)$ is not expected to differ significantly from $E_{rot}(H_3^+)$. Consequently, the 120 K $E_{rot}(H_2D^+)$ is an extrapolation between $E_{rot}(H_2D^+)$ at 100 K and $E_{rot}(H_3^+)$ at 140 K. The subsequent asterisked values of $E_{rot}(H_2D^+)$ are as calculated for H_3^+.

imum value of -115 K at $T = 115$ K and then rising to a maximum value of -235 K at 0 K. The form of the curve in Figure 1 is comparable to that reported by us previously except that the present values of $-\Delta H/R$ are approximately 4–9 K larger.

Our previously determined value of $\Delta H = -(90 \pm 10)$ K at 80 K for reaction 5 is smaller than the calculated value of -125 K. As discussed in previous papers, this is due to the excess rotational energy of the reactant species in the VT-SIFT at 80 K which can drive the endothermic reverse reaction,[13,16,17] thus lowering the experimentally determined value of K_{eq}.

The entropy change in these reactions can also be calculated as a function of temperature using the expression for the individual entropies, S, of the species[37]

$$S = k_B \ln (q_{r-n}q_t) + k_B T \frac{\delta \ln (q_{r-n}q_t)}{\delta T} \qquad (14)$$

where q_t, the translational partition function per unit volume is given by[38]

$$q_t = \frac{1}{h^3}(2\pi m k_B T)^{3/2} \qquad (15)$$

where h is Planck's constant and m is the mass of the molecule. Expressions 11, 14, and 15 can be combined to give the expression for the equilibrium constant, K_{eq} (eq 4), as presented in the Introduction. The K_{eq} calculated from this expression are presented in Table II for all the reactions and were obtained using the data in Table III.

The q_{r-n} for the H_2D^+ and HD_2^+ ions could not be calculated accurately at 300 K using expression 4 due to lack of information regarding the higher energy rotational levels. Consequently the 300 K values of q_{r-n} for these ions have been calculated using the expression[44]

$$q_{r-n} = \left(\frac{\pi^{1/2}}{\sigma}\right)\left(\frac{k_B T}{hc}\right)^{3/2}\left(\frac{1}{ABC}\right)^{1/2} \qquad (16)$$

where the constants have the usual meaning, σ is the symmetry number of the ion, and A, B, and C are the rotational constants of the ion. This expression is quite accurate for species in which the rotational energy level spacings are much less than $k_B T$ but represents only an approximation for species with large rotational energy level spacings. The q_{r-n} for H_3^+ and D_3^+ calculated at 300 K using expression 16 are 5 and 3% smaller, respectively, than the q_{r-n} calculated using expression 12. Thus the individual q_{r-n} for H_2D^+ and HD_2^+ are likely to be in error by <5% as obtained by expression 16 at 300 K.

The experimental values of K_{eq} ($=k_f/k_r$) determined at 300 K are in excellent agreement with those calculated using expression 4. Note that, although the calculated K_{eq} refer to the condition for which there is equilibrium between the nuclear spin states of the species, the reactant species are essentially in their equilibrium nuclear spin distributions at 300 K even though interconversion is not occurring at a significant rate. The experimental values of K_{eq} at 80 K are in general significantly smaller than the calculated values. Quantitatively, this is not unexpected since, as stated earlier, the reactants in the VT-SIFT have excess rotational energy at 80 K (due to noninterconversion of the nuclear spin states) which can enhance the reverse (endothermic) reactions, thus leading to erroneously low experimentally determined values of K_{eq} (and hence ΔH). It is unlikely that the forward reaction rate coefficients are affected significantly by the excess rotational energy since this direction is exothermic.

Interestingly, differential reactivity of the various nuclear spin states of the ions was not observed in either the exothermic or endothermic reactions at 300 or 80 K. A possible explanation is that the difference in the rotational energy content of the ions with different nuclear spin configurations is not sufficient to make an experimentally observable effect on the reaction kinetics.

The lack of agreement between the experimentally determined K_{eq} and the calculated K_{eq} at 80 K raises the question of the validity of using k_f/k_r as an equilibrium constant for these $H_3^+ + H_2$ series of reactions. The nonequilibration of the nuclear spin states of the reactant species below 300 K imply that all reactions occur under nonequilibrium conditions. Consequently, one cannot strictly use a van't Hoff plot to extract ΔH and ΔS since such a procedure necessitates equilibrium conditions. However, using some assumptions, it may be possible to extract information on the relative reactivity of the molecules in their individual spin states by comparison of the calculated K_{eq} with the experimentally determined values of k_f/k_r.[16].

Conclusions

In general, the experimentally observed kinetics in the $H_3^+ + H_2$ series of reactions can be understood in a quantitative manner through a knowledge of the zero-point energies of the reactant and product species.

The agreement between the experimentally determined equilibrium constants and those calculated at 300 K indicates that when the reactants are in true equilibrium in the VT-SIFT, k_f/k_r represents a true equilibrium constant. However, at temperatures much below 300 K, the reactant species do not equilibrate rotationally to the kinetic temperature, leading to erroneously low experimental values of equilibrium constants as compared to the calculated values. Indeed, for the $H_3^+ + H_2$ system of reactions, the ratio k_f/k_r does not represent a true equilibrium constant at temperatures below 300 K in the VT-SIFT.

Acknowledgment. We thank Dr. J. P. Huke and Dr. R. A. Kennedy for many useful discussions on the statistical mechanics. Further, N.G.A. and D.S. thank the SERC (UK) for funding this work and K.G. acknowledges the award of a SERC research studentship.

References and Notes

(1) McMahon, T. B.; Miasek, P. G.; Beauchamp, J. L. *Int. J. Mass Spectrom. Ion Phys.* **1976**, *21*, 63.
(2) Smith, D. L.; Futrell, J. H. *Chem. Phys. Lett.* **1976**, *40*, 229.
(3) Gentry, W. R. In *Gas Phase Ion Chemistry*; Bowers, M. T., Ed.; Academic Press: New York, 1979; Vol. 2, p 221.
(4) Henchman, M. J.; Adams, N. G.; Smith, D. *J. Chem. Phys.* **1981**, *75*, 1201.
(5) Smith, D.; Adams, N. G.; Alge, E. *J. Chem. Phys.* **1982**, *77*, 1261.
(6) Grabowski, J. J.; DePuy, C. H.; Bierbaum, V. M. *J. Am. Chem. Soc.* **1983**, *105*, 2565.
(7) Squires, R. R.; Bierbaum, V. M.; Grabowski, J. J.; DePuy, C. H. *J. Am. Chem. Soc.* **1983**, *105*, 5185.
(8) Lias, S. G. *J. Phys. Chem.* **1984**, *88*, 4401.

(9) Smith, D.; Adams, N. G. In *Ionic Processes in the Gas Phase*; Almoster-Ferreira, M. A., Ed.; D. Reidel: Dordrecht, 1984; p 41.
(10) Grabowski, J. J.; DePuy, C. H.; Bierbaum, V. M. *J. Am. Chem. Soc.* **1985**, *107*, 7384.
(11) Hansel, A.; Richter, R.; Lindinger, W.; Ferguson, E. E. *Int. J. Mass Spectrom. Ion Processes* **1989**, *94*, 251.
(12) Graul, S. T.; Brickhouse, M. D.; Squires, R. R. *J. Am. Chem. Soc.* **1990**, *112*, 631.
(13) Adams, N. G.; Smith, D. *Astrophys. J.* **1982**, *263*, 123.
(14) Brown, R. D.; Rice, E. *Philos. Trans. R. Soc. London A* **1981**, *303*, 523.
(15) Smith, D. *Philos. Trans. R. Soc. London A* **1981**, *303*, 535.
(16) Herbst, E. *Astron. Astrophys.* **1982**, *111*, 76.
(17) Smith, D.; Adams, N. G.; Alge, E. *Astrophys. J.* **1982**, *263*, 123.
(18) Dalgarno, A.; Lepp, S. *Astrophys. J.* **1984**, *287*, L47.
(19) Crutcher, R. M.; Watson, W. D. In *Molecular Astrophysics*; Diercksen, G. H. F., Ed.; D. Reidel: Dordrecht, 1985; p 255.
(20) Brown, R. D.; Rice, E. H. N. *Mon. Not. R. Astron. Soc.* **1986**, *223*, 429.
(21) Herbst, E.; Adams, N. G.; Smith, D.; DeFrees, D. J. *Astrophys. J.* **1987**, *312*, 351.
(22) Wootten, A. In *Astrochemistry*; Vardya, M. S., Tarafdar, S. P., Eds.; D. Reidel: Dordrecht, 1987; p 311.
(23) Henchman, M. J.; Paulson, J. F.; Smith, D.; Adams, N. G.; Lindinger, W. In *Rate Coefficients in Astrochemistry*; Millar, T. J., Williams, D. A., Eds.; Kluwer Academic: Dordrecht, 1988; p 201.
(24) Millar, T. J.; Bennett, A.; Herbst, E. *Astrophys. J.* **1989**, *340*, 906.
(25) Pineau des Forets, G.; Roueff, E.; Flower, D. R. *Mon. Not. R. Astron. Soc.* **1989**, *240*, 167.
(26) Pineau des Forets, G.; Flower, D. R.; McCarroll, R. *Mon. Not. R. Astron. Soc.* **1991**, *248*, 173.
(27) Atkins, P. W. *Physical Chemistry*, 3rd ed.; Oxford University Press: Oxford, U.K., 1988; Chapter 28.
(28) Atkins, P. W. *Physical Chemistry*, 3rd ed.; Oxford University Press: Oxford, U.K., 1988; Chapter 10.
(29) Woodward, L. A. *Molecular Statistics for Students of Chemistry*; Clarendon Press: Oxford, U.K., 1975; Chapter 7.
(30) Smith, D.; Adams, N. G. *Adv. Atom. Mol. Phys.* **1987**, *24*, 1.
(31) Glasstone, S. *Thermodynamics for Chemists*; Van Nostrand Co. Inc.: New York, 1947; Chapter 6.
(32) Fowler, R. A.; Guggenheim, E. A. *Statistical Thermodynamics*; Cambridge University Press: London, 1949; Chapter 3.
(33) Huber, K. P.; Herzberg, G. *Molecular Spectra and Molecular Structure IV: Constants of Diatomic Molecules*; Van Nostrand Reinhold: New York, 1979.
(34) Meyer, W.; Botschwina, P.; Burton, P. *J. Chem. Phys.* **1986**, *84*, 891.
(35) Henchman, M.; Smith, D.; Adams, N. G. *Int. J. Mass Spectrom. Ion Processes* **1991**, *109*, 105.
(36) Huntress Jr., W. T.; Anicich, V. G. *Astrophys. J.* **1976**, *208*, 237.
(37) Woodward, L. A. *Molecular Statistics for Students of Chemistry*; Clarendon Press: Oxford, U.K., 1975; Chapter 5.
(38) Woodward, L. A. *Molecular Statistics for Students of Chemistry*; Clarendon Press: Oxford, U.K., 1975; Chapter 6.
(39) Watson, J. K. G.; Foster, S. C.; McKellar, A. R. W.; Bernath, P.; Amano, T.; Pan, F. S.; Crofton, M. W.; Altman, R. S.; Oka, T. *Can. J. Phys.* **1984**, *62*, 1875.
(40) Foster, S. C.; McKellar, A. R. W.; Peterkin, I. R.; Watson, J. K. G.; Pan, F. S.; Crofton, M. W.; Altman, R. S.; Oka, T. *J. Chem. Phys.* **1986**, *84*, 91.
(41) Foster, S. C.; McKellar, A. R. W.; Watson, J. K. G. *J. Chem. Phys.* **1986**, *85*, 664.
(42) Watson, J. K. G.; Foster, S. C.; McKellar, A. R. W. *Can. J. Phys.* **1987**, *65*, 38.
(43) Carney, G. D.; Porter, R. N. *J. Chem. Phys.* **1977**, *66*, 2756.
(44) Atkins, P. W. *Physical Chemistry*, 3rd ed.; Oxford University Press: Oxford, U.K., 1988; Chapter 10.

Time-Resolved Infrared Studies of Gas-Phase Coordinatively Unsaturated Photofragments $(\eta^5\text{-}C_5H_5)Mn(CO)_x$ (x = 2 and 1)

Youfeng Zheng, Wenhua Wang, Jingu Lin, Yongbo She, and Ke-Jian Fu*

Institute of Physics, Chinese Academy of Sciences, P.O. Box 603, Beijing 100080, People's Republic of China
(Received: February 3, 1992; In Final Form: June 9, 1992)

Time-resolved infrared spectroscopy is used to study the coordinatively unsaturated species $(\eta^5\text{-}C_5H_5)Mn(CO)_x$ (x = 2 and 1) generated by 266- and 355-nm laser photolysis of $(\eta^5\text{-}C_5H_5)Mn(CO)_3$ in the gas phase. $(\eta^5\text{-}C_5H_5)Mn(CO)$ is the predominant photoproduct upon 266-nm photolysis while both $(\eta^5\text{-}C_5H_5)Mn(CO)$ and $(\eta^5\text{-}C_5H_5)Mn(CO)_2$ are produced upon 355-nm photolysis. IR spectra in the region of 1820–2033 cm^{-1} are assigned for the coordinatively unsaturated species $(\eta^5\text{-}C_5H_5)Mn(CO)_x$ and found to be in major disagreement with those obtained in condensed phases. The rate constants for the reactions of $(\eta^5\text{-}C_5H_5)Mn(CO)_2$ and $(\eta^5\text{-}C_5H_5)Mn(CO)$ with CO are determined to be $(5.9 \pm 0.4) \times 10^{11}$ and $(6.7 \pm 0.2) \times 10^{12}$ cm^3 mol^{-1} s^{-1}, respectively. The rate constant for the reaction of $(\eta^5\text{-}C_5H_5)Mn(CO)$ with CO is on the order of 1/10 gas kinetic while the corresponding value for $(\eta^5\text{-}C_5H_5)Mn(CO)_2$ is over an order of magnitude smaller. The magnitudes of the rate constants for the reactions of $(\eta^5\text{-}C_5H_5)Mn(CO)_x$ with CO are compared with those of $(\eta^6\text{-}C_6H_6)Cr(CO)_x$ previously observed and are discussed in terms of the change of spin states of these reactions. In addition, it is found that the presence of rare gas Q (Q = Ar, He, and Xe) has remarkable influence on the kinetic behavior of $(\eta^5\text{-}C_5H_5)Mn(CO)_2$, implying the formation of rare-gas complexes $(\eta^5\text{-}C_5H_5)Mn(CO)_2\cdot Q$ in the gas phase.

I. Introduction

Coordinatively unsaturated transition-metal carbonyl compounds are of primary importance in the elucidation of mechanisms of various systems.[1] Several techniques have been developed toward the identification and characterization of these short-lived, highly reactive species.[2-4] Flash photolysis with time-resolved IR spectroscopy is regarded as a powerful technique in studying the structure and reactivity of coordinatively unsaturated metal carbonyl species in both solution and the gas phases.[3,4] Application of this technique in the gas phase is particularly useful since gas-phase studies offer the opportunity to provide the detailed information of the structure and reactivity of these species free from the disturbance of host matrix or solvent molecules.[4]

An extraordinarily rich chemistry is currently developing around the coordinatively unsaturated fragment $(\eta^5\text{-}C_5H_5)Mn(CO)_2$.[5] There has been a large body of experimental investigations[6-14] as well as theoretical calculations[15,16] concerning this species. $(\eta^5\text{-}C_5H_5)Mn(CO)_2$ was first postulated as an intermediate in the photochemical substitution of $(\eta^5\text{-}C_5H_5)Mn(CO)_3$.[6] It has since been generated and characterized following UV photolysis of $(\eta^5\text{-}C_5H_5)Mn(CO)_3$ in low-temperature rare-gas matrices[7,8] and frozen hydrocarbon glasses.[9-11] The more highly unsaturated species $(\eta^5\text{-}C_5H_5)Mn(CO)$ has also been observed upon prolonged UV photolysis of $(\eta^5\text{-}C_5H_5)Mn(CO)_3$ in hydrocarbon glasses.[10] More recent time-resolved studies of UV flash photolysis of $(\eta^5\text{-}C_5H_5)Mn(CO)_3$ in alkane solution at room temperature provided the structure and kinetic information of the solvated species $(\eta^5\text{-}C_5H_5)Mn(CO)_2\cdot S$ (S = solvent).[12,13] It was found that in *n*-heptane solution the rate constant for the reaction of $(\eta^5\text{-}C_5H_5)Mn(CO)_2\cdot S$ with CO is about 10 times smaller than the corresponding value for the reaction of $Cr(CO)_5\cdot S$ with CO in cyclohexane solution.[12,13]

* To whom correspondence may be addressed.

0022-3654/92/2096-7650$03.00/0